ingegneria sismica
International Journal of Earthquake Engineering
Anno XLIII - Num. 1 - 2026

Frequency response characteristics and optimization design method of high-frequency power lines for transmitting electric wave signals

Yunzhe Liu[1,*]

[1] School of Earth and Space Science and Technology, Wuhan University, Wuhan, Hubei, 430000, China

SUMMARY: *There are two kinds of fading models for large and small scale fading in the propagation process of electromagnetic waves, and this paper analyzes the root-mean-square delay expansion and Les K factor of two kinds of small scale fading characteristics under line-of-sight and non-line-of-sight scenarios channels by combining the statistical method with the fitting. A channel model library is established, and multiple large-scale fading models are used to compare the residual sum of squares and the goodness of fit to analyze the large-scale fading characteristics in HF signal transmission. Combined with the performance of the characteristics existing in HF signal transmission, we propose a wireless channel multipath identification algorithm based on D-S evidence theory, analyze the algorithm operation flow, and test the algorithm for multi-channel scene identification. The CDF of the rms delay extensions under the line-of-sight and non-line-of-sight scene channels can be fitted well with shape parameters of 0.727 and 0.272 and scale parameters of 655.33 and 1173.83, respectively. The CDFs of the Rice K factors for the 2 scenarios fit the normal distribution well, with standard deviations less than 3 dB. The wireless channel multipath identification algorithm based on D-S evidence theory can improve the wireless signal transmission identification and optimize the frequency response of wireless signal transmission.*

KEYWORDS: *HF signal transmission; small-scale fading; large-scale fading; D-S evidence; root-mean-square delay expansion; les k factor; wireless channel identification*

1 Introduction

High-frequency wires are an important branch of electronic science and technology, which usually refers to wires working in the radio frequency or microwave frequency band, and the design of these wires involves physical phenomena such as propagation, reflection, and transmission of electric wave signals [1, 2]. High-frequency wires play a key role in many fields such as modern communications and electronic equipment, and the quality of signal transmission directly affects the performance of the entire system [3, 4]. In order to achieve efficient, stable and accurate signal transmission, it is necessary to optimize the frequency response characteristics of high-frequency wires to transmit wave signals.

The optimization of high-frequency wires requires not only the consideration of basic wire parameters, but also an in-depth understanding of electromagnetic field theory and signal integrity issues [5, 6]. The transmission line is the channel for signal transmission in high-frequency wires, and its characteristics have a significant impact on signal transmission [7]. It is important to select the appropriate type of transmission line according to the actual needs.

*Lyz747805@163.com
https://doi.org/10.65102/is2026123
Published: 30 April, 2026

Microstrip lines, on the other hand, are commonly used for signal transmission inside integrated circuits or on printed circuit boards, which have the advantages of easy integration and lower cost. In terms of transmission line design, it is crucial to consider the matching of characteristic impedance [8, 9]. Mismatch of characteristic impedance will lead to signal reflection, loss of energy of the transmitted signal, and waveform distortion. In addition, when calculating the characteristic impedance, factors such as the geometry of the transmission line and the dielectric material should be considered comprehensively. By precisely calculating and adjusting these parameters, the characteristic impedance of the transmission line matches the input and output impedance of the connected circuit components, thus reducing signal reflection and ensuring efficient signal transmission. The length of the transmission line also needs to be strictly controlled [10]. Excessively long transmission lines increase signal transmission delay and attenuation, and when designing high-frequency wires, the length of the transmission line should be shortened as much as possible to avoid unnecessary detours and excessively long alignments [11, 12].

This paper briefly analyzes the radio wave signal propagation mechanism, shadow fading, and the loss phenomenon existing in radio wave signal propagation. Based on the ITU frequency allocation standard, the basic elements of high-frequency signal transmission are clarified. Two parameters, root-mean-square delay extension and Rice K factor in small-scale fading are extracted to analyze the parameter fitting under the channel of line-of-sight and non-line-of-sight scenarios. A channel model library is established by selecting various models including free-space model and logarithmic distance path loss model, and translational distance, residual sum of squares, and goodness-of-fit R^2 are computed to analyze the large-scale fading of HF signal propagation. Propose a wireless channel multipath identification algorithm based on D-S evidence theory and analyze the channel scene identification rate of the algorithm.

2 Radio wave propagation

2.1 Radio wave propagation

Wave propagation in the wireless environment from the transmitter-side antenna to the receiver-side consists of direct (i.e., free-space) waves, reflected waves, bypassed waves, and scattered waves.

(1) Direct wave

Free space propagation is electromagnetic wave propagation in an ideal propagation medium space, will not produce refraction, reflection, absorption and scattering and other phenomena, will only occur due to energy dispersion of electromagnetic waves caused by the propagation path attenuation, the classic free space propagation of microwave line-of-sight communications and satellite communications. In free space propagation, assuming that P_t represents the transmitter spherical wave EIRP, i.e., the transmit power of omnidirectional radiation, and P_r represents the received power, there are:

$$P_r = P_t\left(\frac{\lambda}{4\pi d}\right)^2 g_t g_r \tag{1}$$

where g_t and g_r denote the gain of the transceiver antenna, λ denotes the wavelength, and d denotes the straight line distance between the receiving and transmitting antennas, respectively.

The free space propagation loss can be defined as:

$$L_s = \frac{P_t}{P_r} = \left(\frac{4\pi d}{\lambda}\right)^2 \frac{1}{g_t g_r} \tag{2}$$

Losses are often expressed in decibels, then:

$$L_s = 32.45 + 20\log d + 20\log f - 10\log\left(g_t g_r\right) \tag{3}$$

When $g_t = g_r = 1$, then:

$$L_{bs} = 32.45 + 20\log d + 20\log f \tag{4}$$

where d denotes distance in kilometers. f denotes the frequency in megahertz. L_{bs} denotes the propagation path loss, which refers to the propagation path loss of two ideal antennas (with gain coefficient $g_t = g_r = 1$) in free space.

(2) Reflected waves

Electromagnetic waves in a variety of propagation medium overlap, the phenomenon of reflection. Electromagnetic wave reflection in the ideal propagation medium surface is no energy loss, the reflection coefficient (i.e., the incident wave than the reflected wave field strength) R is equal to 1. If the electromagnetic wave propagation to the surface (ideal propagation medium), some energy will be transmitted to the new medium to continue propagation, and some other energy will be reflected in the original medium.

If the electromagnetic wave propagates to the surface of the reflector (ideal reflector), then all the energy will be reflected back, at this time the incident wave field strength and the reflected wave field strength ratio R for 1, that is, the reflection coefficient. In the case of a non-ideal propagation medium, the reflection coefficient $R = \left(\sin\theta - z\right)/\left(\sin\theta + z\right)$, and z means that when the antenna adopts a vertical polarization: $z = \sqrt{\varepsilon_0 - \cos^2\theta}\big/\varepsilon_0$, and when the antenna is horizontally polarized: $z = \sqrt{\varepsilon_0 - \cos^2\theta}$. $\varepsilon_0 = \varepsilon - j60\sigma\lambda$, where θ denotes the angle of incidence, ε denotes the permittivity of the reflecting medium, σ denotes the conductivity of the reflecting medium, and λ denotes the wavelength.

The propagation schematic is shown in Fig. 1, the electromagnetic wave propagates through direct and reflection to the point B received signal strength P_r is:

$$P_r \approx P_t\left(\frac{\lambda}{4\pi d}\right)^2 g_t g_r \left|1 + \mathrm{Re}^{(-j\Delta\Phi)}\right|^2 \tag{5}$$

where the phase difference $\Delta\Phi = \frac{2\pi\Delta l}{\lambda}$ and $\Delta l = \left(AC + CB\right) - AB$. Then the multipath propagation model can be expressed as:

$$P_r = P_t\left(\frac{\lambda}{4\pi d}\right)^2 g_t g_r \left|1 + \sum_{i=1}^{n} R_i e^{(-j\Delta\Phi_i)}\right|^2 \tag{6}$$

Assuming that there are many paths number n when different with the formula correctly

calculated on the received signal Pr, so the above formula of the formula only theoretical derivation, so through the above formula is also can not be calculated by the actual propagation mode, calculation of the actual received signal only use the method of statistics.

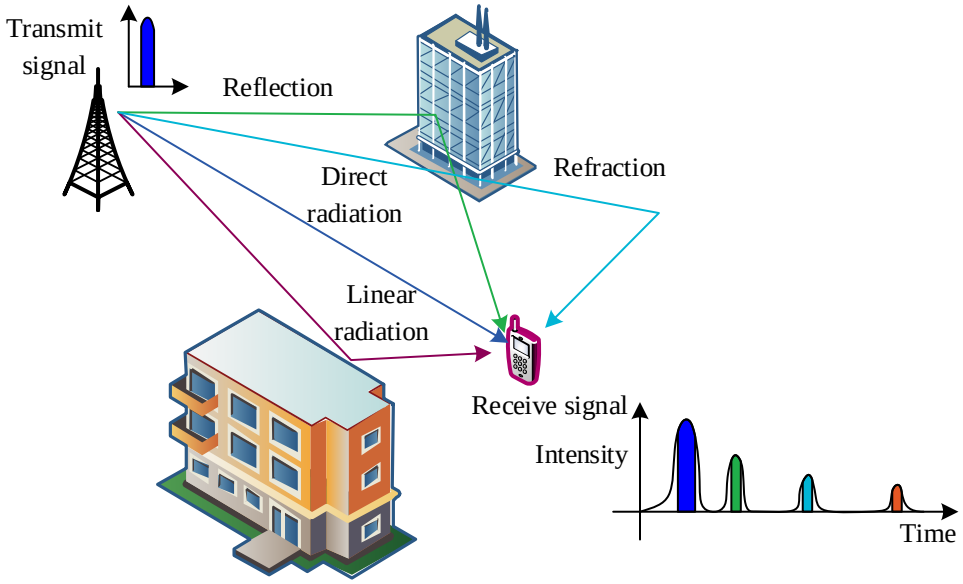

Figure 1: Propagation diagram

(3) Wave bypassing

Bypassing field strength is the ability of a radio wave to bypass an obstruction and form a field strength behind the obstruction. According to Huygen's law: this is because the points located in front of the obstruction will act as a new source to transmit a spherical secondary wave, this secondary wave in the back of the obstruction to form the field strength of the region, that is, bypassed wave field.

(4) Scattered wave

Scattered wave refers to a wireless propagation system in which the size of the signal at the receiving point is larger than that predicted by both the orbiting and reflecting wave models described above. Because when the radio wave encounters a rough surface obstacle will be reflected, to all around the signal will be reflected, that is, the scattering phenomenon.

2.2 Shadow Decay

When the location of the receiving point is changed at any time, it will pass through a variety of height, location, area size is not consistent with the blocking object, but these blocking objects are not consistent with each other's straight-line distance. Thus, the signal strength received at the receiving point is inconsistent, the signal average value of the random change, this phenomenon is shadow fading.

Since the shadow fading almost does not change with time, only with the path loss, regional geomorphology, weather and frequency correlation, so the shadow fading is the key to the propagation model calibration, the final calibration results are also mainly affected by the shadow fading.

The propagation path loss can be expressed as:

$$l(r,\zeta) = r^m 10^{(\zeta/10)} \tag{7}$$

Shadow decay can be expressed as:

$$10\log l(r,\zeta) = 10m\log r + \zeta \tag{8}$$

where r denotes the distance between the transmitter and receiver, ζ denotes the logarithmic loss (shadow generation) in dB, which satisfies a normal distribution with mean 0 and standard deviation σdB, and m denotes the path loss exponent. Therefore the shadow fading will obey the lognormal distribution.

2.3 Radio wave propagation losses

Since the propagation process of wireless electromagnetic wave is mainly affected by the propagation environment, the study of wireless propagation model must be combined with the propagation environment. In the propagation process of electromagnetic wave from the transmitting antenna to the receiving antenna, due to the complexity of the propagation environment, multiple propagation paths will be generated. And the farthest distance that electromagnetic wave can propagate is determined by the path loss generated in the propagation process.

In the process of electromagnetic wave propagation, there are two kinds of fading models, large and small scale fading model. If the propagation distance between the transmitting antenna and the receiving antenna is more than one hundred meters, the change of the received signal strength can be described by the large-scale propagation model. If the propagation distance is several times the wavelength or the propagation time is in the second level, then the small-scale propagation model should be used to describe, so the intensity of the received signal changes very quickly.

(1) Large-scale fading model

Path loss and shadow fading are the main characteristics of the large-scale fading model. Among them, the path loss is caused by the frequency of the transmitting antenna, the electromagnetic wave propagation distance, and the terrain in the propagation process, etc. The shadow fading is caused by the sudden drop of the received signal in some areas due to the obstruction of buildings or terrain features encountered in the propagation process.

(2) Small-scale fading model

Multipath fading is the main characteristic of the small-scale propagation model. As electromagnetic waves in the propagation process, reflection, bypassing and scattering phenomena, which leads from the transmitting antenna to the receiving antenna propagation path is more than one, that is to say, the receiving antenna will receive a number of different received signals, and these signals are not the same arrival time and signal strength.

(3) Multipath effect

When the location of the transmitting antenna and receiving antenna changes, the electromagnetic wave propagation path will change accordingly, the corresponding propagation path will change, the path loss will also change, reflected in the value is the amplitude of the received signal will change. At the same time, due to changes in multiple propagation paths, the time delay to the receiving antenna will also change accordingly.

3 HF signal propagation frequency response characteristics

3.1 Electromagnetic spectrum

Radio wave frequency range is 3Hz~3000GHz, different frequencies of radio waves have different propagation characteristics, the actual work is often based on the work of the frequency band to select the appropriate propagation method for radio propagation.

According to the different propagation characteristics and application services, the International Telecommunication Union (ITU) has divided the entire radio spectrum into very low frequency (VLF), low frequency (LF), intermediate frequency (IF), high frequency (KF), very high frequency (VHF), ultra-high frequency (UHF), ultra-high frequency (UHF), extra-high frequency (EHF), extreme high frequency (EHF), and high frequency (KF), and the corresponding bands are very ultra-long wave (VULW), long wave (LW), intermediate wave (IW), short wave (SHW), meter wave (mW), decimeter wave (dW), centimeter wave (CM), millimeter wave (mmW), and micron wave (μW). The shorter the wavelength, the more information can be transmitted in the same time.

According to the ITU Frequency Allocation Standard, the frequency range of high frequency (HF) is from 3 MHz to 30 MHz and the wavelength range is from 100m to 10m.

3.2 Small Scale Fading Characterization

Small-scale fading generally refers to the rapid change in signal field strength over short distances or short periods of time. The 2 parameters, Root Mean Square Delay Expansion (RMS-DS) and Rice K factor, have a large impact on the small-scale fading characteristics. Therefore, this paper analyzes and fits these 2 parameters according to the test channel results, observes the distribution function with the highest fit to the characterization data, and obtains the statistical characteristics of this small-scale fading characteristics, so as to understand the distribution of small-scale fading characteristics more intuitively.

3.2.1 Root Mean Square Delay Expansion

The simulation results of the channel rms delay extension in the line-of-sight scenario are shown in Fig. 2, where the horizontal coordinate is the number of channels obtained by measuring the real environment several times, and the vertical coordinate is the value of the corresponding rms delay extension for each channel.

The maximum value of the channel rms delay extension in the line-of-sight scenario is 4389.81ns, and the average value is 972.04ns.

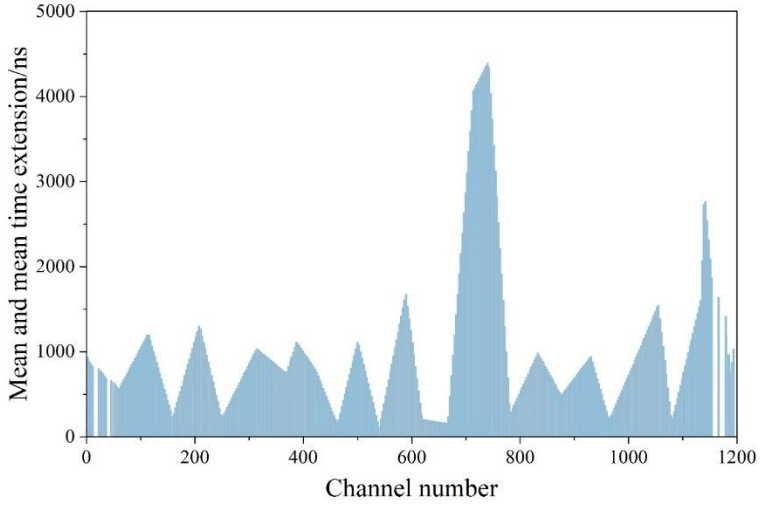

Figure 2: The distance of the sight distance is the time delay extension simulation value

The simulation results of the channel rms delay extension for the non-line-of-sight scenario are shown in Fig. 3, where the maximum value is 4880.87ns and the average value is 3178.07ns.

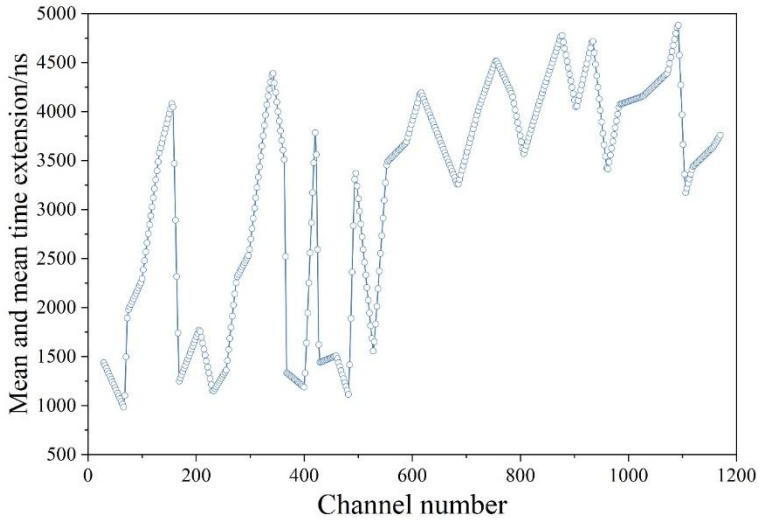

Figure 3: Non-stave-oriented scenario channel simulation results

The RMS-DS measurements and fitting results are shown in Fig. 4, which shows a comparison of the cumulative distribution function (CDF) of the RMS-DS for the 2 scenarios. The CDFs of the RMS delay extensions for the 2 scenarios both fit the Gamma distribution well, with shape parameters of 0.727 and 0.272, and scale parameters of 655.33 and 1173.83, respectively.

The RMS-DS probability densities were calculated for these 2 scenarios, and the fitted plots show that in the line-of-sight scenario, about 65% of the RMS-DS values are within 150 ns. About 7% of the RMS-DS values are greater than 1000 ns. In the non-line-of-sight scenario, the minimum RMS-DS value is greater than 150 ns and more than 80% of the RMS-DS values are greater than 1000 ns.

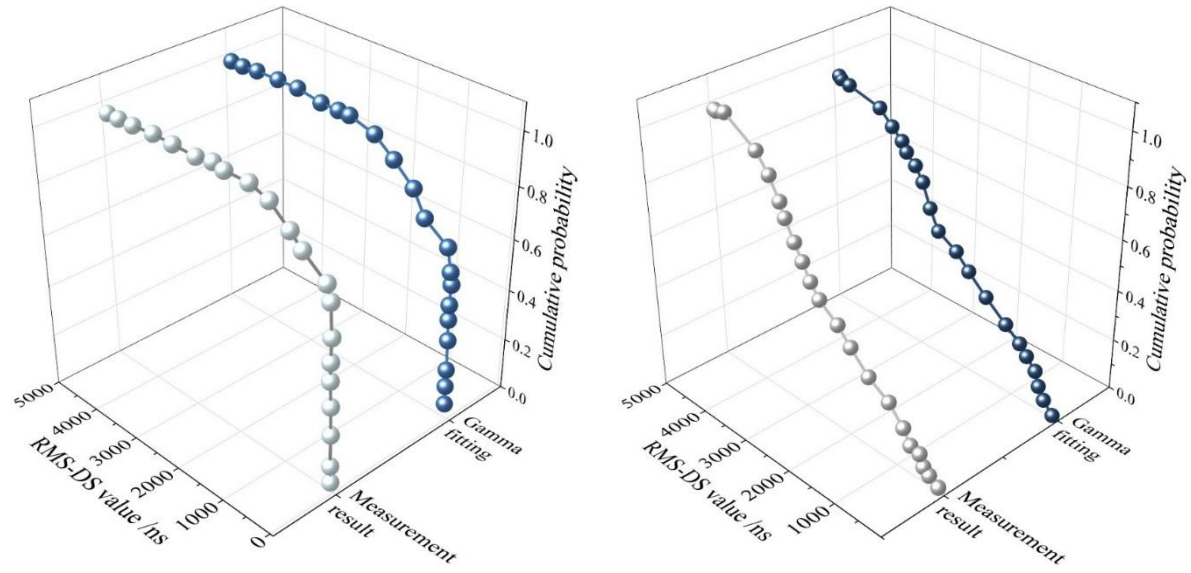

(a) Stadia scenario (b) Non-stadia scenario

Figure 4: Rms-ds measurements and fitting results

3.2.2 Rice K-factor

In this paper, we obtain the values of the Rice factor in 2 environments by calculating the channel measurement data and compare the CDF fitting results. The Rice K factor measurement and fitting results are shown in Fig. 5, Figs. (a) and (b) are for the non-line-of-sight scenario and the line-of-sight scenario, respectively, where the CDFs of the Rice K factor in the 2 scenarios are well fitted to the normal distribution, and the standard deviation of the Rice K factor in the 2 scenarios is less than 3 dB.

Calculating the probability density of the Rice K-factor under the two scenarios, the mean value of the Rice K-factor under the line-of-sight scenario is larger than that of the non-line-of-sight scenario, which is about 4 dB and 0.5 dB, respectively, which is opposite to the trend of the RMS-DS value transformation, which is due to the fact that there are fewer buildings in the line-of-sight scenario, and the propagation environment is relatively wide, whereas the non-line-of-sight scenario has more buildings and the propagation environment is complex.

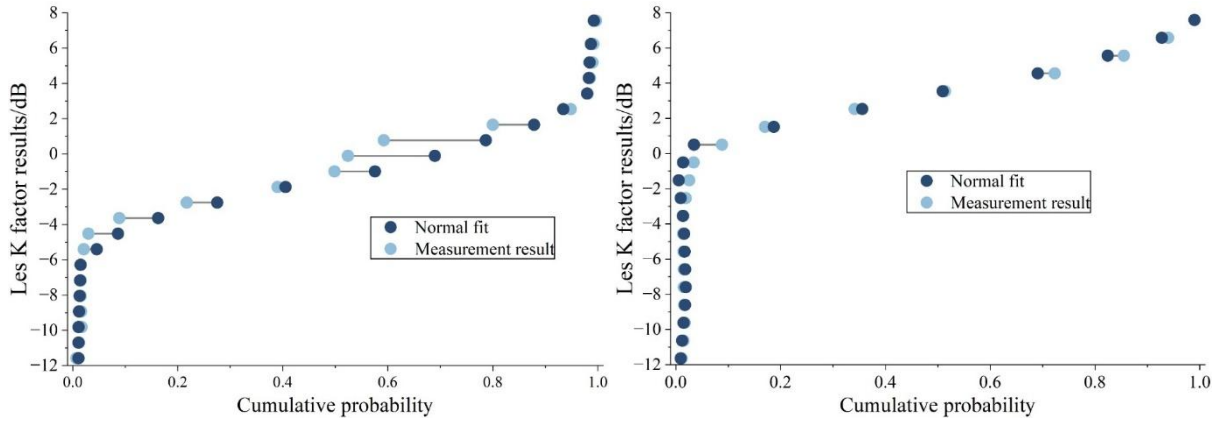

(a) Non-stadia scenario (b) Stadia scenario

Figure 5: Rice K factor measurement and fitting result

3.3 Large-scale decay characterization

A channel model library is established to analyze the large-scale fading of HF signal propagation by fitting the loss of the large-scale channel model and the measured data by calculating the residual sum of squares and the goodness-of-fit.

3.3.1 Establishment of channel model library

The channel model library includes a variety of typical channel models, this channel model library is constructed under the MATLAB platform, and the selected model can be directly plotted with the signal propagation loss distance curve of the model, and the test data in the actual environment can be visually compared with each model in the channel model library, which is very helpful for the rapid determination and correction of the channel model of wireless communication.

This model library consists of a free space model, a two-path model, a logarithmic distance path loss model, a logarithmic normal shadow loss model, and a flat earth model. The channel model library includes three parts: model parameter module, model function module, and interface display module. The model parameter module is located in the interface and consists of transmit signal frequency, transmit power, transceiver antenna gain, transceiver antenna height, cable loss and simulation distance. The model function module consists of functions of each model, and each model function has a model file. The interface display module is used to plot model curves and measured data curves.

3.3.2 Characterization of test data

After the measured data are processed, the data are loaded into the channel model library to obtain the loaded data channel model library. Through the simulation model library, it can be seen that under the same input parameters, the prediction results of each model have obvious differences, this paper will be up and down shifted and analyze each model by calculating the residual sum of squares and goodness-of-fit R^2, resulting in the model library after the shifting. It can be seen that, except for the two-path model, the trends of the other models do not differ significantly, so this paper analyzes each model by calculating the residual sum of squares and goodness-of-fit R^2. The residual sum of squares and goodness of fit of each path loss model are shown in Table 1. It can be seen that the logarithmic distance path loss model has the smallest residual sum of squares, 207.819, and the highest goodness of fit, 0.996.

Table 1: The square of the two squares of the model and the optimal degree of the match

Translation modified model	Free space model	Logarithmic distance loss model	Logarithmic normal shadow loss model	Two-path model	Plane earth model
Translation distance(dB)	11	34	36	-91	-161
Residual sum of squares	326.213	207.819	261.005	6235.995	512.407
Fitting excellence R^2	0.992	0.996	0.996	0.878	0.964

4 Wireless channel porous measurements and data analysis

4.1 Wireless channel multipath identification based on D-S evidence

4.1.1 D-S theory of evidence

In the $D-S$ theory of evidence, a set can be called an identification frame if elements of the set can be interpreted as the answer to a particular question and this answer is the only correct answer to the question. The identification frame in this theory is the set of all possibilities for events and objects, and any elements in it are independent of each other, and at any given time, the possibility of an event can only be an element of the set. Let Θ be the set of all possibilities for the event X to exist taking values where the number of elements is finite, e.g.:

$$\Theta=\left\{x_1,x_2,x_3,\cdots,x_i,\cdots,x_N\right\} \tag{9}$$

where Θ is the signal recognition framework of $D-S$ evidence theory, x_i is one of all possibilities of event X, N is the number of all possibilities of event X, $i=1,2,\cdots,N$.

Any elements in the signal recognition framework Θ of the $D-S$ evidence theory are independent of each other, and the set consisting of all subsets of the signal recognition framework Θ together is known as the power set, denoted 2^{Θ}, as in:

$$2^{\Theta}=\left\{\phi,\left\{x_1\right\},\left\{x_2\right\},\cdots,\left\{x_N\right\},\left\{x_1\cup x_2\right\},\left\{x_1\cup x_3\right\},\cdots,\Theta\right\} \tag{10}$$

When there are a total of N sub-elements in the signal recognition framework Θ, then the power set has a total of 2^N sub-elements, and any element A in the power set will correspond to the proposition that the likelihood of an event X is said to be the proposition that "the value of X exists in a sub-element A of the power set".

In the framework of the identification of $D-S$ theories of evidence, a 2^{Θ} to $[0,1]$ is a mapping and satisfies:

$$\begin{cases} m(\phi)=0 \\ \sum\limits_{A\subseteq\Theta} m(A)=1 \end{cases} \tag{11}$$

is then called the basic probability assignment (BPA) function, also known as the mass function. A denotes a subset of the recognition framework Θ. $m(A)$ is the basic assignment function of A that indicates the level of confidence in A and makes A with $m(A)>0$ a focal element. The $m(\phi)=0$ indicates that the trust in the null evidence is 0.

In the recognition framework Θ, A denotes any subset of the recognition framework Θ and B is any subset of A, then B is also a subset of the recognition framework Θ. A 2^{Θ} to $[0,1]$ is a mapping and satisfies:

$$Bel(A)=\sum_{B\subseteq A} m(B) \tag{12}$$

Then $Bel(A)$ is the trust function for A, also known as the confidence function.

The basic distribution function is the degree of trust in a set, but does not include the degree of trust in any of the subsets of that set, so the basic distribution function is a partial trust in the evidence. Unlike the basic distribution function, the confidence function can be used to represent the degree of confidence in a set or subset of a set, i.e., the confidence function can be used to represent the global degree of confidence in the evidence.

In $D-S$ theory of evidence, if only use A trust function to represent the degree of trust for A, this for A degree of trust for the representation of a hint of insufficiency, so in the $D-S$ theory of evidence is also introduced into the likelihood function, used to represent the degree of suspicion for A. In $D-S$ evidence theory of identification framework Θ, A is any subset of the framework, and can be expressed as:

$$pl(A)=1-Bel(\bar{A})=\sum_{B\subseteq\Theta}m(B)-\sum_{B\subseteq\bar{A}}m(B)=\sum_{B\cap A\neq\phi}m(B) \tag{13}$$

where $\bar{A}=\Theta-A$, then $pl(A)$ is known as the likelihood function, which takes values in the range $[0,1]$.

$Bel(\bar{A})$ denotes the degree of trust in the set $\bar{A}$, i.e., the degree of trust that the set A is false, and thus $pl(A)$ denotes the degree of trust that the set A is non-false, and $pl(A)>Bel(A)$. For the subset A in the $D-S$ evidence-theoretic identification framework Θ, the $Bel(A)$ and $pl(A)$ of A can be computed by utilizing the basic distribution function of the subset A, and then $[Bel(A),pl(A)]$ is the trust interval for A, indicating the degree of trust for A.

4.1.2 Overall flow of multipath recognition algorithm

Based on the correlation of static measurement data, this section proposes a wireless channel multipath identification algorithm based on D-S evidence theory for identifying high-order multipath signals, and the overall flow of the algorithm is shown in Fig. 6.

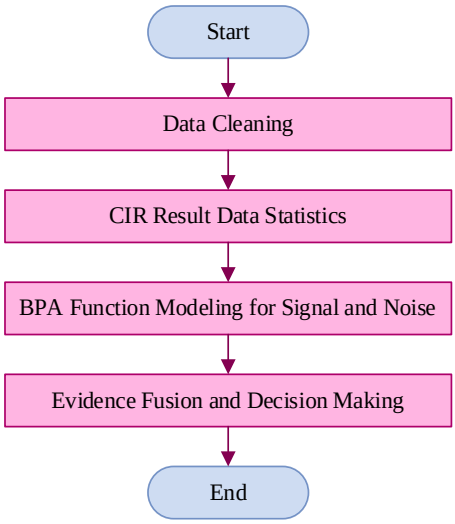

Figure 6: The overall process of the multipath recognition algorithm

(1) BPA function model of signal and noise

Since the distribution of the channel impulse response resultant statistic X_i conforms to a Gaussian distribution, the signal and noise basic distribution function models can be obtained using the cumulative distribution function of the Gaussian distribution:

$$m_i\left(H_0\right)=\frac{2}{\sqrt{2\pi}\sigma_m}\int_{X_i}^{+\infty}\exp\left(-\frac{\left(x-\mu_m\right)^2}{2\sigma_m^2}\right)dx \tag{14}$$

$$m_i\left(H_1\right)=\frac{2}{\sqrt{2\pi}\sigma_m}\int_{0}^{X_i}\exp\left(-\frac{\left(x-\mu_m\right)^2}{2\sigma_m^2}\right)dx \tag{15}$$

where H_0 denotes the noise determined based on the CIR analysis results, H_1 denotes the signal determined based on the CIR analysis results, $m_i\left(H_0\right)$ is the BPA function of the noise, $m_i\left(H_1\right)$ is the signal's BPA function, X_i is the CIR analysis result, and σ_m^2 and μ_m are the maximum likelihood estimates of the variance and mean of the CIR result, respectively.

(2) Evidence fusion and decision making

For the CIR analysis results in the same measurement scenario, the BPA function values of the signal and noise corresponding to a certain transmission delay in one of the sets of acquired data corresponding to the CIR results are derived according to Eqs. (14) and (15). Then, following the same procedure, the basic distribution functions of signal and noise corresponding to the CIR results for the same transmission delay in the other data sets are derived sequentially. And for all the basic allocation functions of signal and noise corresponding to the same transmission delay, the weights between them are calculated using the evidence distance to realize the evidence fusion, and the basic allocation functions of signal and noise after fusion are obtained. Finally, the judgment is performed according to the evidence decision rule to obtain the final signal and noise judgment results, i.e:

$$R=\begin{cases}1, m\left(H_1\right)\geq m\left(H_0\right)\\ 0, m\left(H_1\right)< m\left(H_0\right)\end{cases} \tag{16}$$

where 1 represents the verdict as signal, 0 represents the verdict as noise, $m\left(H_1\right)$ is the underlying distribution function of the signal after evidence fusion, and $m\left(H_0\right)$ is the underlying distribution function of the noise after evidence fusion.

4.2 Channel Scene Recognition

Simulation methods for Rayleigh channels include sinusoidal superposition and formation filter methods. Although the design complexity of the formation filter is higher, its statistical accuracy is higher than that of the sinusoidal superposition method, and it can better simulate the fading channel. Therefore, the formation filter method used in this paper models five types of Rayleigh fading channels, namely, Rayleigh-Classical, Rayleigh-Gaussian, Rayleigh-Flat, Rayleigh-Butterworth, and Rayleigh-Domed Arch, respectively.

The sampling frequency is set to 50kHz, the random number seed is *'mt*19937*ar with seed'*, seed is 40, the maximum Doppler shift is set to 600Hz, and the channel length is 300,000 points to generate the five types of fading channel data.

The Anderson-Darling test is used to analyze the amplitude envelopes and phases of the first-order statistical characteristics of the five Rayleigh channel models, and the AR model spectral estimation method is used to extract the channel power spectra, selecting to obtain the channel data whose average absolute error meets the requirements and whose first-order statistical characteristics meet the requirements of the channel scenarios, and conducting 100 Monte Carlo simulations for each type of fading channel, extracting the channel second-order statistical characteristics power spectrum data as the training and testing dataset.

The five channel scenarios are recognized using the wireless channel multipath recognition algorithm based on D-S evidence theory proposed in this paper, and the recognition results of different algorithms are shown in Fig. 7.The Gaussian distribution algorithm performs the best in the face of the Rayleigh-Classical channel model recognition, but the recognition rate of the Rayleigh-Butterworth channel model is 0.714.The recognition rates of three algorithms for the Rayleigh-Classical channel model are all 90% Above that, the wireless channel multipath recognition algorithms based on D-S evidence theory have high recognition accuracy for all five scenarios, and the algorithms all have a good recognition rate of 90% or more.

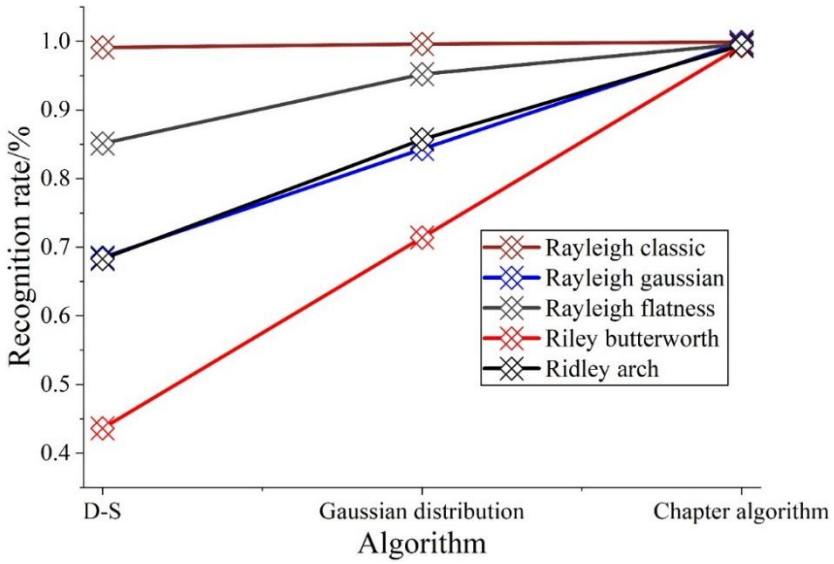

Figure 7: Identification of different algorithms

5 Conclusion

In this paper, we analyze the effects of small-scale fading and large-scale fading on the propagation of HF signals, and propose a wireless channel multipath identification algorithm based on the D-S evidence theory to enhance the transmission identification of multipath signals and optimize the frequency response of HF signal transmission.

(1) Small-scale fading is important for the quality of wireless communication, which is affected by multipath propagation and Doppler effect. Small-scale fading is susceptible to root-mean-square (RMS) delay extension and Rice K factor, and the maximum values of RMS delay extension for line-of-sight scene channel and non-line-of-sight scene channel in the simulation environment are 4389.81ns and 4880.87ns, respectively, while the average values are 972.04ns and 3178.07ns. The CDFs of the Rice K-factors for both the nonline-of-sight and line-of-sight scenarios fit the normal distribution well, and the standard deviations of the Rice K-factors are all less than 3 dB.

(2) There is large-scale fading in HF signal propagation, and the translation distance,

residual sum of squares, and goodness-of-fit R^2 are calculated using the free-space model, the logarithmic distance path loss model, the log-normal shadowing loss model, the two-path model, and the planar earth model, among which the logarithmic distance path loss model has the best results for large-scale fading processing.

(3) The wireless channel multipath identification algorithm based on D-S evidence theory can successfully identify five types of Rayleigh fading channel models, namely, Rayleigh-Classical, Rayleigh-Gaussian, Rayleigh-Flat, Rayleigh-Butterworth, and Rayleigh- Circular-Arch, and improves the quality of frequency response of HF signal transmission.

References

[1] Barrios, E. L., Ursua, A., Marroyo, L., & Sanchis, P. (2014). Analytical design methodology for litz-wired high-frequency power transformers. IEEE Transactions on Industrial Electronics, 62(4), 2103-2113.

[2] Yip, P. (2012). High-frequency circuit design and measurements. Springer Science & Business Media.

[3] Singh, H. (2021, October). A review on high frequency communication. In 2021 2nd International Conference on Smart Electronics and Communication (ICOSEC) (pp. 1722-1727). IEEE.

[4] Crepaldi, M., Zini, G., Maviglia, A., Barcellona, A., Merello, A., & Brayda, L. (2017, October). Live wire: Body channel communication as a high impedance and frequency-scaled impulse radio. In 2017 IEEE Biomedical Circuits and Systems Conference (BioCAS) (pp. 1-4). IEEE.

[5] Liu, J., Deng, Q., Czarkowski, D., Kazimierczuk, M. K., Zhou, H., & Hu, W. (2018). Frequency optimization for inductive power transfer based on AC resistance evaluation in litz-wire coil. IEEE Transactions on Power Electronics, 34(3), 2355-2363.

[6] Wojda, R. P., &Kazimierczuk, M. K. (2015). Analytical optimization of litz-wire windings independent of porosity factor. COMPEL: The International Journal for Computation and Mathematics in Electrical and Electronic Engineering, 34(3), 920-940.

[7] Faria, J. A. B., Araneo, R., &Stracqualursi, E. (2023). Surface Wave, Skin Effect, and Per Unit Length Parameters of the Single-Wire Transmission Line at Low Frequency, for Nonmagnetic and Magnetic Wires. IEEE Access, 11, 59621-59635.

[8] Lushchin, S. P., Borkovskih, A. V., &Borkovskih, M. V. (2018). Analysis of electrotechnical properties of innovative high-temperature wires for overhead power transmission lines. Electrical Engineering and Power Engineering, (2), 37-44.

[9] Steckiewicz, A., Zajkowski, M., & Jovanovic, A. (2025). Potential Properties and Applications of Wires with Helical Structure in High-Voltage Overhead Power Lines and PV Systems. Energies, 18(22), 6008.

[10] Chen, C., Yang, H., Wang, W., Mandich, M., Yao, W., & Liu, Y. (2020). Harmonic transmission characteristics for ultra-long distance AC transmission lines based on frequency-length factor. Electric Power Systems Research, 182, 106189.

[11] Azizi, S., Sun, M., Liu, G., Popov, M., &Terzija, V. (2019). High-speed distance relaying of the entire length of transmission lines without signaling. IEEE Transactions on Power Delivery, 35(4), 1949-1959.

[12] Chen, C., Ma, X., Yang, H., Wang, W., & Liu, Y. (2020). Study on the Power-Frequency Waves Distribution Characteristics for Half-Wavelength Transmission Lines Based on the Frequency-Length Factor. Mathematical Problems in Engineering, 2020(1), 3497625.